



Contrast-enhanced ultrasound LI-RADS 2017: comparison with CT/MRI LI-RADS

Jianmin Ding^{1,2} · Lei Long² · Xiang Zhang³ · Chen Chen³ · Hongyu Zhou² · Yan Zhou² · Yandong Wang² · Xiang Jing² · Zhaoxiang Ye¹ · Fengmei Wang⁴

Received: 19 April 2020 / Revised: 14 June 2020 / Accepted: 5 August 2020 / Published online: 15 August 2020
© European Society of Radiology 2020

Abstract

Objective To compare the classification based on contrast-enhanced ultrasound (CEUS) Liver Imaging Reporting and Data System (LI-RADS) with that of contrast-enhanced CT and MRI (CECT/MRI) LI-RADS for liver nodules in patients at high risk of hepatocellular carcinoma.

Methods Two hundred thirty-nine patients with 273 nodules were enrolled in this retrospective study. Each nodule was categorized according to the CEUS LI-RADS version 2017 and CECT/MRI LI-RADS version 2017. The diagnostic performance of CEUS and CECT/MRI was compared. The reference standard was histopathology diagnosis. Inter-modality agreement was assessed with Cohen's kappa.

Results The inter-modality agreement for CEUS LI-RADS and CECT/MRI LI-RADS was fair with a kappa value of 0.319 ($p < 0.001$). The positive predictive values (PPVs) of hepatocellular carcinoma (HCC) in LR-5, LR-4, and LR-3 were 98.3%, 60.0%, and 25.0% in CEUS, and 95.9%, 65.7%, and 48.1% in CECT/MRI, respectively. The sensitivities and specificities of LR-5 for diagnosing HCC were 75.6% and 93.8% in CEUS, and 83.6% and 83.3% in CECT/MRI, respectively. The positive predictive values of non-HCC malignancy in CEUS LR-M and CECT/MRI LR-M were 33.9% and 93.3%, respectively. The sensitivity, specificity, and accuracy for diagnosing non-HCC malignancy were 90.9%, 84.5%, and 85.0% in CEUS LR-M and 63.6%, 99.6%, and 96.7% in CECT/MRI LR-M, respectively.

Conclusions The inter-modality agreement of the LI-RADS category between CEUS and CECT/MRI is fair. The positive predictive values of HCCs in LR-5 of the CEUS and CECT/MRI LI-RADS are comparable. CECT/MRI LR-M has better diagnostic performance for non-HCC malignancy than CEUS LR-M.

Key Points

- The inter-modality agreement for the final LI-RADS category between CEUS and CECT/MRI is fair.
- The LR-5 of CEUS and CECT/MRI LI-RADS corresponds to comparable positive predictive values (PPVs) of HCC. For LR-3 and LR-4 nodules categorized by CECT/MRI, CEUS examination should be performed, at least if they can be detected on plain ultrasound.

Jianmin Ding and Lei Long contributed equally to this work.

✉ Xiang Jing
dr.jingxiang@aliyun.com

✉ Zhaoxiang Ye
yezhaoxiang@163.com

¹ Department of Radiology, National Clinical Research Center for Cancer, Tianjin Key Laboratory of Cancer Prevention and Therapy, Tianjin's Clinical Research Center for Cancer, Tianjin Medical University Cancer Institute and Hospital, Tianjin, China

² Department of Ultrasound, Tianjin Institute of Hepatobiliary Disease, Tianjin Key Laboratory of Artificial Cell, Artificial Cell Engineering Technology Research Center of Public Health Ministry, Tianjin Third Central Hospital, Tianjin 300170, China

³ Department of Radiology, Tianjin Institute of Hepatobiliary Disease, Tianjin Key Laboratory of Artificial Cell, Artificial Cell Engineering Technology Research Center of Public Health Ministry, Tianjin Third Central Hospital, Tianjin 300170, China

⁴ Department of Gastroenterology and Hepatology, Tianjin Institute of Hepatobiliary Disease, Tianjin Key Laboratory of Artificial Cell, Artificial Cell Engineering Technology Research Center of Public Health Ministry, Tianjin Third Central Hospital, Tianjin 300170, China

- *CECT/MRI LR-M has better diagnostic performance for non-HCC malignancy than CEUS LR-M. For LR-M nodules categorized by CEUS, re-evaluation by CECT/MRI is necessary.*

Keywords Carcinoma, Hepatocellular · Ultrasonography · Tomography, Spiral computed · Magnetic resonance imaging · Contrast agent

Abbreviations

| | |
|---------|------------------------------------------------------------|
| ACR | American College of Radiology |
| APHE | Arterial phase hyperenhancement |
| CECT | Contrast-enhanced computerized tomography |
| CEUS | Contrast-enhanced ultrasound |
| CHC | Combined hepatocellular cholangiocarcinoma |
| CPS/CHI | Contrast pulse sequencing/contrast high-resolution imaging |
| EOB-MRI | Gadoxetic acid-enhanced magnetic resonance imaging |
| FN | False negative |
| FP | False positive |
| HCC | Hepatocellular carcinoma |
| HGDN | High-grade dysplastic nodule |
| ICC | Intrahepatic cholangiocarcinoma |
| LGDN | Low-grade dysplastic nodule |
| LI-RADS | Liver Imaging Reporting and Data System |
| LR | Likelihood ratio |
| M | Metastases |
| NPV | Negative predictive value |
| PI | Pulse inversion imaging |
| PPV | Positive predictive value |
| RN | Regenerative nodule |
| TN | True negative |
| TP | True positive |

Introduction

Detection of hepatocellular carcinoma (HCC) at early stage is important for patients at risk of HCC. Contrast-enhanced computerized tomography (CECT), gadoxetic acid-enhanced magnetic resonance imaging (EOB-MRI), and contrast-enhanced ultrasound (CEUS) are the three most widely used diagnostic modalities for HCC [1]. However, many challenges still remain. In order to provide a standardized categorization and interpretation, the American College of Radiology (ACR) established the Liver Imaging Reporting and Data System (LI-RADS) in 2011 [2]. LI-RADS was originally designed for multi-phase enhanced CT/MRI. Following the demonstration of CEUS diagnostic performance [3, 4], the ACR developed CEUS LI-RADS in 2016, updated in 2017 [5, 6].

Both CEUS and CECT/MRI LI-RADS are developed to categorize liver nodules in patients at high risk. However, comparison between CEUS LI-RADS and CECT/MRI LI-

RADS for categorization has not been well achieved. This study was designed to compare CEUS LI-RADS version 2017 and CECT/EOB-MRI LI-RADS version 2017 for the categorization performance for patients at high risk of HCC.

Materials and methods

This study was approved by the Ethics Committee of Tianjin Third Central Hospital. Informed consent was waived. Patients at high risk of HCC who underwent CEUS and CECT or EOB-MRI from June 2017 to January 2019 (Fig. 1) in our institution were included in this study. Liver histology, including ultrasound-guided biopsy and surgical pathology, served as the standard reference. The inclusion criteria were (1) patients at high risk of HCC with complete imaging data; (2) nodules detected by US and CECT/EOB-MRI; (3) nodule number ≤ 3 ; (4) nodules with pathological diagnosis; and (5) an interval of less than 4 weeks between CEUS and CECT/EOB-MRI examinations. The patients with the following criteria were excluded: (1) no HCC risk factor identified; (2) cirrhosis due to congenital hepatic fibrosis; (3) cirrhosis due to a vascular disorder; (4) multiple regenerative hyperplasia nodules or diffuse HCC; (5) local progression of nodules after treatment.

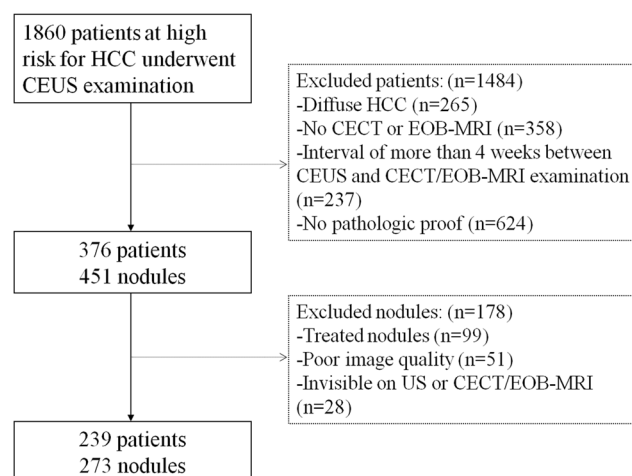


Fig. 1 Flowchart of patient selection

CEUS

US images were obtained by Philips EPIQ 7 ultrasound system (Philips Medical System) equipped with a C5-1 (1.0–5.0 MHz) convex array probe, pulse inversion imaging (PI) software, and mechanical index 0.04–0.08, or by Acuson S3000 ultrasonic diagnostic system (Siemens Medical Solutions) equipped with a 6C1HD (1.0–6.0 MHz) convex array probe, contrast pulse sequencing/contrast high-resolution imaging (CPS/CHI) software, and mechanical index 0.08–0.10. The sulfur hexafluoride microbubble (SF₆) contrast agent (SonoVue, Bracco) was sufficiently mixed with 5 ml saline before bolus injection in the antecubital vein. The conventional and color Doppler US was performed to record the number, location, size, shape, pattern of internal echo, and blood flow distribution of liver nodules. Images were captured in a standard manner, including all liver segments, with the participants placed in supine and left lateral decubitus positions. Livers were evaluated during quiet respiration. The section of nodules at the largest cross-sectional view was selected for contrast imaging acquisition. After intravenous injection of 1.2 to 2.0 ml of contrast agent through the antecubital vein, followed by a flush of 5 ml 0.9% sodium chloride solution, the imaging of target lesion was recorded for 60 s. After 60 s, the

lesion was intermittently scanned and recorded for 5 min to characterize washout features. All images were saved and then analyzed frame by frame.

CT

Dynamic CECT scanning was performed with the patients placed at supine position by using Somatom Definition Flash dual-energy CT (Siemens Medical Solutions). A contrast agent (iohexol, 350 mg/ml, Beilu Pharmaceutical Co., Ltd.), at a dosage of 1.2 ml/kg body weight and a flow rate of 3.5 ml/s, was injected with a pressure injector via the median cubital vein. An automatic bolus-tracking technique was used. The hepatic arterial phase imaging acquisition started with a delay of 25 s to 35 s after the threshold had been reached. The portal venous phase imaging acquisition started at about 50 s to 70 s after the initiation of contrast injection, and the late phase was at about 180 s after the initiation of contrast injection.

MRI

EOB-MR imaging was performed with Siemens Magnetom Verio 3.0-T magnetic resonance unit (Siemens Medical Solutions), using phased array surface coils. Liver MR imaging protocol consisted of in-phase and opposed-phase T1-weighted imaging, FSE T2-weighted imaging with fat suppression, and diffusion-weighted imaging. For EOB-DTPA-enhanced imaging, 0.025 mmol/kg gadoteric acid (Primovist; Bayer Healthcare) was intravenously injected at a rate of 1.0 ml/s by using a power injector, followed by 25-ml saline flush. Arterial, portal venous, and transitional phase images were acquired at the delay time of 15 to 18 s and 50 to 60 s, 180 s after contrast injection using volumetric interpolated breath-hold examination (VIBE) sequence. Hepatobiliary phase imaging was completed 20 min after the contrast injection.

Table 1 Clinical characteristics of patients and nodules

| Characteristic | Value |
|----------------------------|-----------------------|
| Patient (<i>n</i> = 239) | |
| Mean age (year)* | 59.1 ± 8.0 |
| Sex | |
| Male | 182 |
| Female | 57 |
| Known cirrhosis | 205 |
| Etiology of liver disease | |
| Hepatitis B virus | 195 (82) |
| Hepatitis C virus | 20 (8) |
| Alcohol | 9 (4) |
| Autoimmune hepatitis | 8 (3) |
| Other causes | 7 (3) |
| No. of nodules per patient | |
| 1 | 208 (87) |
| 2 | 28 (12) |
| 3 | 3 (1) |
| Nodule (<i>n</i> = 273) | |
| Nodule size (mm)* | |
| CEUS | 3.07 ± 1.94 (1.0–6.1) |
| CT/MRI | 2.85 ± 1.89 (1.0–5.5) |

Unless stated otherwise, data are number of patients or nodules. Data in parentheses are percentages

*Data are mean ± standard deviation

Table 2 Comparison of the results between CEUS and CECT/EOB-MRI classification

| CEUS category | CECT/EOB-MRI category | | | | Total |
|---------------|-----------------------|---------|-----------|--------|-----------|
| | 3 | 4 | 5 | M | |
| 3 | 10 (1) | 4 (1) | 2 (2) | 0 | 16 |
| 4 | 6 (1) | 13 (8) | 6 (6) | 0 | 25 |
| 5 | 10 (10) | 11 (11) | 152 (149) | 0 | 173 |
| M | 1 (1) | 7 (3) | 36 (31) | 15 (1) | 59 |
| Total | 27 | 35 | 196 | 15 | 273 (225) |

Unless stated otherwise, data are number of nodules. Data in parentheses are number of HCCs

Image analysis

All CEUS images were independently reviewed by two radiologists (J.M.D. and H.Y.Z., with more than 11 years and 6 years of experience in liver CEUS, respectively). Each nodule was categorized based on the CEUS LI-RADS version 2017. To resolve discrepancies between the two observers, images were re-evaluated together with assistance of the third, more experienced radiologist (X.J., with 15 years of experience in hepatic imaging and CEUS) until a consensus was reached. All CECT/EOB-MRI images were reviewed by X.Z. and C.C., with more than 20 and 15 years of experience in abdominal imaging. Each nodule was categorized based on the CECT/EOB-MRI LI-RADS version 2017, including major and ancillary imaging features of the nodules [7]. For patients who received both CECT and EOB-MRI examinations, the nodules were classified according to EOB-MRI data. In case of discrepancy with regard to the nodule category assignment, an additional experienced radiologist (Z.X.Y., with more than 30 years of experience) was involved to provide the arbitration. All the radiologists were blinded to the pathologic results and other imaging findings.

Statistical analysis

Quantitative data was expressed as $\bar{x} \pm SD$ (mean \pm SD), and categorical variables were expressed by frequency. To evaluate the diagnostic performance of the US LI-RADS in the detection of HCC, the accuracy, sensitivity, specificity, positive predictive value (PPV), and negative predictive value (NPV) were calculated. Comparison between subgroups was achieved using the paired chi-square test. The Cohen's kappa coefficient was used for the evaluation of inter-modality agreement. Statistical analyses were performed using SPSS software, version 17.0 (SPSS Inc.).

Results

Participant characteristics

A total of 239 patients, including 182 males and 57 females, were included. The median age was 56 years ranging from 22 to 80 years. Two hundred seventy-three nodules include 225 HCCs, 8 combined hepatocellular cholangiocarcinomas (CHCs), 12 intrahepatic cholangiocarcinomas (ICCs), 2 metastases (M), and 26 benign nodules. A total of 181 nodules were confirmed by biopsy and 92 nodules were confirmed by surgical pathology. Among the 273 nodules, 125 nodules underwent CECT examination, 94 nodules underwent EOB-MRI examination, and 54 nodules underwent both EOB-MRI and CECT examinations. The basic clinical characteristics of patients and nodules are shown in Table 1.

CEUS and CECT/EOB-MRI LI-RADS

The percentages of nodules in LR-5, LR-4, LR-3, and LR-M for CEUS LI-RADS were 63.3%, 9.2%, 5.9%, and 21.6%, and for CECT/EOB-MRI LI-RADS, 71.8%, 12.8%, 9.9%, and 5.5%, respectively (Table 2). Inter-modality agreement for CEUS LI-RADS and CECT/EOB-MRI LI-RADS was fair ($\kappa = 0.319$, $p < 0.001$, Fig. 2, Fig. 3). The results of classification by CEUS LI-RADS and CECT/EOB-MRI LI-RADS for the nodules and their pathological diagnosis are shown in Table 3.

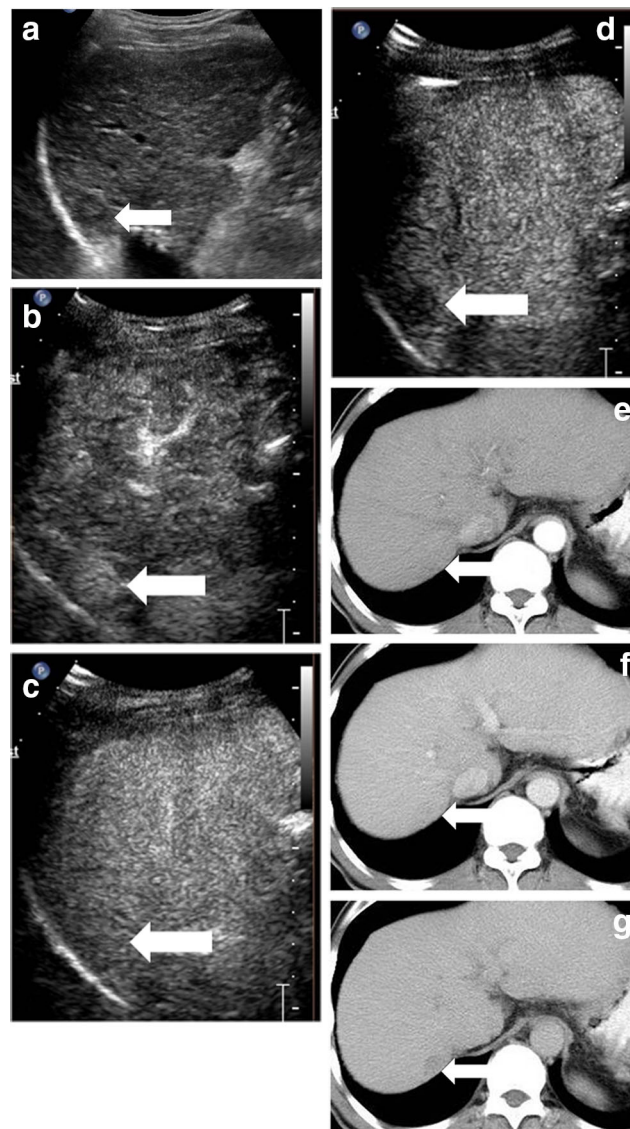


Fig. 2 A well-differentiated HCC lesion in S7 was categorized as LR-5 by CEUS and LR-3 by CECT in a 55-year-old man with chronic HBV infection and cirrhosis. **a** Ultrasound imaging revealed a 15-mm hypoechoic observation. CEUS: **b** showed arterial phase hyperenhancement, **c** without washout in the portal venous phase, **d** followed by mild washout in the delayed phase. CECT: **e** showed iso-enhancement in the arterial phase, **f** no washout in the portal venous phase, **g** washout in the delayed phase

The diagnostic performance of CEUS and CECT/EOB-MRI LI-RADS

Among the 273 nodules, the PPVs of HCCs for CEUS LI-RADS and CECT/EOB-MRI LI-RADS were 98.3% (170/173, 95% CI: 94.6%, 99.6%) vs. 95.9% (188/196, 95% CI: 91.8%, 98.1%) in LR-5; 60.0% (15/25, 95% CI: 38.9%, 78.1%) vs. 65.7% (23/35, 95% CI: 47.7%, 80.3%) in LR-4; and 25.0% (4/16, 95% CI: 0.8%, 52.6%) vs. 48.1% (13/27, 95% CI: 29.2%, 67.6%) in LR-3, respectively. No statistically significant difference of PPV was found between CEUS LR-5 and CECT/EOB-MRI LR-5 (Table 4). Two CHCs were assigned into CEUS LR-5 and no ICC was assigned into CEUS LR-4 or LR-5. However, two ICCs were assigned into the CECT/MRI LR-4 and LR-5, three CHCs were assigned into the LR-4 CECT/MRI, and four CHCs were assigned into the CECT/MRI LR-5.

The diagnostic performances for non-HCC malignancies of CEUS LR-M and CECT/EOB-MRI LR-M are shown in

Table 4. The PPV for non-HCC hepatic malignancies of CEUS LR-M was 33.9% (20/59, 95% CI: 22.4%, 47.5%), and that of CECT/EOB-MRI LR-M was 93.3% (14/15, 95% CI: 66.0%, 99.7%), respectively ($p = 0.000$). The diagnostic accuracy for non-HCC hepatic malignancies of CEUS LR-M was 85.0% (95% CI: 80.1%, 88.9%) and that of CECT/EOB-MRI LR-M was 96.7% (95% CI: 93.6%, 98.4%), respectively ($p = 0.000$). The incidence of HCCs in CEUS LR-M was 61.0% (36/59). For the 36 HCCs classified as CEUS LR-M, 31 HCCs were categorized as LR-5 (Fig. 4), 3 HCCs were categorized as LR-4, and 1 HCC was categorized as LR-3 by CECT/EOB-MRI. One HCC was classified as LR-M by both CEUS and CECT/EOB-MRI.

Discussion

The result of this study showed that the inter-modality agreement for the final LI-RADS category between CEUS and

Fig. 3 A HCC lesion in S7 was categorized as LR-5 by CEUS and LR-4 by EOB-MRI in a 49-year-old man with chronic HBV infection and cirrhosis. Ultrasound revealed a 31-mm hypo-echoic observation. CEUS: **a** showed arterial phase hyperenhancement, **b** no washout in the portal venous phase, **c** mild washout in the delayed phase; EOB-MRI: **d** showed hyperenhancement in the arterial phase, **e** slight hyperenhancement in the portal venous phase, **f** hypo-intensity in the hepatobiliary phase

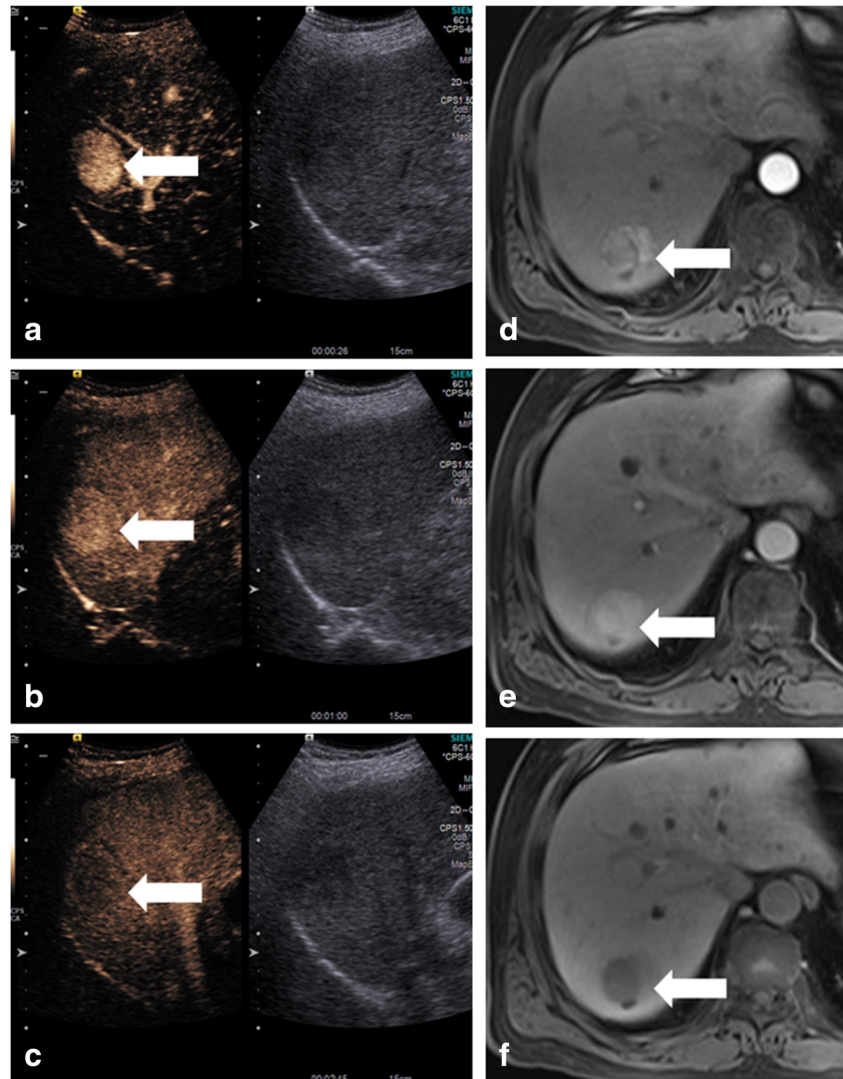


Table 3 Comparison of pathological results and category between CEUS and CECT/EOB-MRI

| Category | CEUS | | | | | CECT/EOB-MRI | | | | |
|--------------|------|----|-----|----|-------|--------------|----|-----|----|-------|
| | 3 | 4 | 5 | M | Total | 3 | 4 | 5 | M | Total |
| HCC | 4 | 15 | 170 | 36 | 225 | 13 | 23 | 188 | 1 | 225 |
| ICC | 0 | 0 | 0 | 12 | 12 | 0 | 1 | 1 | 10 | 12 |
| CHC | 0 | 0 | 2 | 6 | 8 | 0 | 1 | 5 | 2 | 8 |
| Metastases | 0 | 0 | 0 | 2 | 2 | 0 | 0 | 0 | 2 | 2 |
| RN | 1 | 2 | 0 | 0 | 3 | 2 | 1 | 0 | 0 | 3 |
| LGDN | 6 | 1 | 0 | 1 | 8 | 4 | 4 | 0 | 0 | 8 |
| HGDN | 4 | 6 | 1 | 0 | 11 | 7 | 3 | 1 | 0 | 11 |
| Inflammation | 1 | 0 | 0 | 2 | 3 | 1 | 1 | 1 | 0 | 3 |
| Hemangioma | 0 | 1 | 0 | 0 | 1 | 0 | 1 | 0 | 0 | 1 |
| Total | 16 | 25 | 173 | 59 | 273 | 27 | 35 | 196 | 15 | 273 |

Unless stated otherwise, data are number of nodules. *HCC* hepatocellular carcinoma, *ICC* intrahepatic cholangiocarcinoma, *CHC* combined hepatocellular cholangiocarcinoma, *RN* regenerative nodule, *LGDN* low-grade dysplastic nodule, *HGDN* high-grade dysplastic nodule

CECT/EOB-MRI was fair ($\kappa = 0.319$), similar to the result of Schellhaas et al [7]. CEUS enables real-time, dynamic, and continuous observation of nodule enhancement pattern, while CECT/MRI only scans at fixed time points, which may miss capturing wash-in [6, 8, 9]. The CEUS contrast agent is a pure blood pool contrast agent which does not diffuse into the intercellular space and has advantages of producing real and obvious washout [6, 8, 9]. Both CT and MRI contrast agents are extracellular which diffuse into the extracellular space and deposit in the matrix [6, 8, 9]. In addition, CEUS LR-5 had a high specificity (93.3%) and PPV for the diagnosis of HCC

(98.3%), which was consistent with the previous studies [10, 11]. A systematic review including 17 retrospective studies reported that among 3556 nodules, the PPV for HCCs of CECT/MRI LR-5 was 94%, similar to that in our study (95.9%). In addition, the phenomenon in the present work that ICC was misclassified into LR-5 was also mentioned in a previous study [12].

The discordance between CEUS and CECT/EOB-MRI for LR-3 and LR-M was analyzed in our study. LR-3 is assigned to findings that have a moderate probability of being HCC or a benign entity. In previous studies, the PPVs for HCCs in the LR-3 category ranged from 15 to 60% in CEUS [11, 13], and 20–70% in CECT/MRI [14]. In this study, the PPVs for HCC of CEUS LR-3 and CECT/EOB-MRI LR-3 were 25.0% and 48.1%, respectively. It has been mentioned that the risk of HCC in CEUS LR-3 is higher than that of CECT/MRI LR-3 [8]. In the present study, however, the PPV for HCCs in LR-3 was lower in CEUS than that in CECT/EOB-MRI. Firstly, all nodules in this study were ultrasonically visible, namely “real nodules.” “Fake nodules,” such as the artery-portal venous shunt (APS), possibly mistakenly classified as LR-3 on CECT/EOB-MRI, were not included in this study [6, 14, 15]. Secondly, due to the different mechanisms of the two imaging modalities, CEUS is more sensitive in detecting arterial phase hyperenhancement (APHE) than CECT/MRI, especially compared with EOB-MRI [1, 8]. Our previous research has shown that CEUS has a good diagnostic accuracy for early HCC whose most important feature is APHE [16]. The classification of HCC without the arterial phase hyperenhancement determined by CECT/EOB-MRI LR-3 may be upgraded by CEUS. Thus, the probability of risk prediction of HCCs in CEUS LR-3 was lower than that in CECT/EOB-MRI LR-3. Therefore, for LR-3 and LR-4 nodules categorized by CECT/MRI, CEUS examination should

Table 4 Comparison of diagnostic performance of LR-5 and LR-M category between CEUS and CECT/EOB-MRI

| Variable | HCC | | Non-HCC malignancies | | | |
|-----------------|-------------------|-------------------|----------------------|-------------------|-------------------|----------------|
| | CEUS LR-5 | CECT/EOB-MRI LR-5 | <i>p</i> value | CEUS LR-M | CECT/EOB-MRI LR-M | <i>p</i> value |
| TP | 170 | 188 | | 20 | 14 | |
| TN | 45 | 40 | | 212 | 250 | |
| FP | 3 | 8 | | 39 | 1 | |
| FN | 58 | 37 | | 2 | 8 | |
| Sensitivity (%) | 75.6 (69.3, 81.0) | 83.6 (77.9, 88.0) | 0.035 | 90.9 (69.4, 98.4) | 63.6 (40.8, 82.0) | 0.031 |
| Specificity (%) | 93.8 (81.8, 98.4) | 83.3 (69.2, 92.0) | 0.109 | 84.5 (79.2, 88.6) | 99.6 (97.4, 99.9) | 0.000 |
| PPV (%) | 98.3 (94.6, 99.6) | 95.9 (91.8, 98.1) | 0.186 | 33.9 (22.4, 47.5) | 93.3 (66.0, 99.7) | 0.000 |
| NPV (%) | 45.0 (35.1, 55.2) | 51.9 (40.3, 63.4) | 0.359 | 99.1 (96.3, 99.8) | 96.9 (93.8, 95.6) | 0.121 |
| LR+ | 12.1 | 5.0 | | 5.9 | 159.7 | |

Data in parentheses are quantitative value of 95% confidence interval

TP true positive, *TN* true negative, *FP* false positive, *FN* false negative, *PPV* positive predictive value, *NPV* negative predictive value, *LR* likelihood ratio

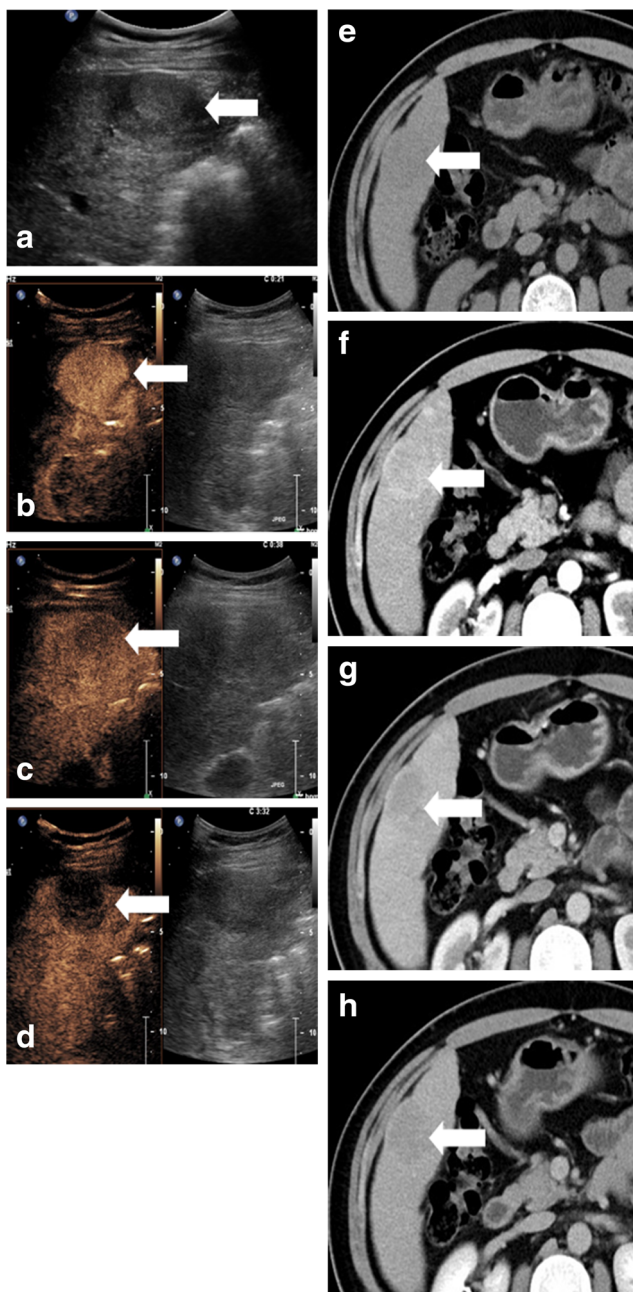


Fig. 4 A moderately and poorly differentiated HCC lesion in S5 was categorized as LR-M by CEUS and LR-5 by CECT in a 40-year-old man with chronic HBV infection and cirrhosis. **a** Ultrasound revealed a 35-mm hypo-echoic observation. CEUS: **b** showed arterial phase hyperenhancement, **c** followed by early washout at 38 s, **d** marked washout at 212 s after SonoVue injection. CECT: **e** scan revealed a hypo-density observation, **f** showed hyperenhancement in the arterial phase, **g, h** washout and enhancing capsule in the portal venous phase and delayed phase

be performed to observe enhancement pattern, at least if they can be detected on plain ultrasound.

The criteria for CEUS LR-M are rim hyperenhancement in the arterial phase, or early washout (< 60 s) or marked washout (< 120 s). The diagnostic performance of the criteria that

differentiate HCC and non-HCC malignancy gets much attention in clinical practice. A single-center retrospective study showed that CEUS LR-M had a sensitivity, specificity, and accuracy (97.25%, 87.72%, and 92.38%) slightly higher than those of our study (90.9%, 84.5%, and 85.0%) for the diagnosis of non-HCC malignancy [17]. Our results were similar to those in another study, in which the sensitivity, specificity, and accuracy for diagnosis of non-HCC malignancies were 91%, 88%, and 88% [11]. The PPV of CEUS LR-M for non-HCC malignancy was only 33.9% in our study, which was lower than that of CECT/EOB-MRI LR-M. A total of 61.0% (36/59) of nodules in CEUS LR-M were confirmed as HCCs. Compared with CEUS LR-M, CECT/EOB-MRI LR-M had higher specificity, positive predictive value, and accuracy in diagnosing non-HCC malignancy. It was also mentioned in a previous study that the CECT/MRI LR-M has a better diagnostic performance than CEUS LR-M for non-HCC malignancies [18]. In addition, according to current criteria of CEUS LR-M, many HCCs would be mistakenly classified as CEUS LR-M. Previous studies [19–21] showed that some of the moderately and poorly differentiated HCCs presented an enhancement pattern of “early washout and marked washout” on CEUS. Furthermore, earlier washout was observed in HCCs with a size ≥ 3 cm than in small hepatocellular carcinoma. In this study, the incidence of HCC in CEUS LR-M was 61.0% (36/59), and 35 of the 36 HCCs were classified as LR-4 or LR-5 by CECT or EOB-MRI. Therefore, for LR-M nodules categorized by CEUS, re-evaluation by CECT/EOB-MRI is necessary.

A total of 8 CHCs were included in this study. Six of 8 CHCs (75.0%) were classified as LR-M by CEUS. Only two (25.0%) CHCs were classified as LR-M category by CECT/EOB-MRI. Neither CEUS nor CECT/MRI LI-RADS can clearly distinguish CHCs from HCCs or ICCs, because the enhancement modes of CHC differ. Thus, biopsy is needed to obtain accurate pathological diagnosis [12, 18, 22].

There are several limitations in the present study: (1) Prospective study is needed to validate the inter-modality agreement and diagnostic performance between CEUS and CECT/MRI LI-RADS; (2) LR-1 and LR-2 nodules usually have no pathological diagnosis, and were not included in this study; (3) CECT LI-RADS and EOB-MRI LI-RADS were not analyzed separately.

In conclusion, the inter-modality agreement for CEUS LI-RADS and CECT/EOB-MRI LI-RADS is fair. The CEUS LR-5 and CECT/EOB-MRI LR-5 have a comparable incidence of HCCs. CECT/EOB-MRI LR-M has better diagnostic performance for non-HCC hepatic malignancies than CEUS LR-M.

Acknowledgments The present work was supported by Tianjin Science and Technology Project (No. 17ZXMFSY00050) and Tianjin Science and Technology Project (No. 17ZXMFSY00170).

Funding information The authors state that this work has not received any funding.

Compliance with ethical standards

Guarantor The scientific guarantor of this publication is Xiang Jing.

Conflict of interest The authors of this manuscript declare no relationships with any companies, whose products or services may be related to the subject matter of the article.

Statistics and biometry No complex statistical methods were necessary for this paper.

Informed consent Written informed consent was waived by the Institutional Review Board.

Ethical approval Institutional Review Board approval was obtained.

Methodology

- retrospective
- diagnostic or prognostic study
- performed at one institution

References

1. Lyshchik A, Kono Y, Dietrich CF et al (2018) Contrast-enhanced ultrasound of the liver: technical and lexicon recommendations from the ACR CEUS LI-RADS working group. *Abdom Radiol (NY)* 43:861–879
2. Mitchell DG, Bruix J, Sherman M, Sirlin CB (2015) LI-RADS (Liver Imaging Reporting and Data System): summary, discussion, and consensus of the LI-RADS Management Working Group and future directions. *Hepatology* 61:1056–1065
3. Seitz K, Bernatik T, Strobel D et al (2010) Contrast-enhanced ultrasound (CEUS) for the characterization of focal liver lesions in clinical practice (DEGUM Multicenter Trial): CEUS vs. MRI—a prospective comparison in 269 patients. *Ultraschall Med* 31:492–499
4. Guang Y, Xie L, Ding H, Cai A, Huang Y (2011) Diagnosis value of focal liver lesions with Sonovue-enhanced ultrasound compared with contrast-enhanced computed tomography and contrast-enhanced MRI: a meta-analysis. *J Cancer Res Clin Oncol* 137:1595–1605
5. Kono Y, Lyshchik A, Cosgrove D et al (2017) Contrast enhanced ultrasound (CEUS) liver imaging reporting and data system (LI-RADS): the official version by the American College of Radiology (ACR). *Ultraschall Med* 38:85–86
6. Wilson SR, Lyshchik A, Piscaglia F et al (2018) CEUS LI-RADS: algorithm, implementation, and key differences from CT/MRI. *Abdom Radiol (NY)* 43:127–142
7. Schellhaas B, Hammon M, Strobel D et al (2018) Interobserver and intermodality agreement of standardized algorithms for non-invasive diagnosis of hepatocellular carcinoma in high-risk patients: CEUS-LI-RADS versus MRI-LI-RADS. *Eur Radiol* 28:4254–4264
8. Kim TK, Noh SY, Wilson SR et al (2017) Contrast-enhanced ultrasound (CEUS) liver imaging reporting and data system (LI-RADS) 2017—a review of important differences compared to the CT/MRI system. *Clin Mol Hepatol* 23:280–289
9. Kambadakone AR, Fung A, Gupta RT et al (2018) LI-RADS technical requirements for CT, MRI, and contrast-enhanced ultrasound. *Abdom Radiol (NY)* 43:56–74
10. Terzi E, Iavarone M, Pompili M et al (2018) Contrast ultrasound LI-RADS LR-5 identifies hepatocellular carcinoma in cirrhosis in a multicenter retrospective study of 1,006 nodules. *J Hepatol* 68:485–492
11. Zheng W, Li Q, Zou XB et al (2019) Evaluation of contrast-enhanced US LI-RADS version 2017: application on 2020 liver nodules in patients with hepatitis B infection. *Radiology* 294:299–307
12. Van der Pol CB, Lim CS, Sirlin CB et al (2019) Accuracy of the Liver Imaging Reporting and Data System in computed tomography and magnetic resonance image analysis of hepatocellular carcinoma or overall malignancy—a systematic review. *Gastroenterology* 156:976–986
13. Terzi E, De Bonis L, Leoni S, Benevento F, Granito A, Tovoli F (2017) CEUS LI-RADS are effective in predicting the risk hepatocellular carcinoma of liver nodules. *Dig Liver Dis* 49:e22
14. Mitchell DG, Bashir MR, Sirlin CB (2017) Management implications and outcomes of LI-RADS-2, -3, -4, and -M category observations. *Abdom Radiol (NY)* 43:143–148
15. Piscaglia F, Wilson SR, Lyshchik A et al (2017) American College of Radiology, contrast enhanced ultrasound liver imaging reporting and data system (CEUS LI-RADS) for the diagnosis of hepatocellular carcinoma: a pictorial essay. *Ultraschall Med* 38:320–324
16. Ding J, Zhou Y, Wang Y, Zhou H, Jing X (2017) Clinical value of contrast enhanced ultrasound in differential diagnosis of early hepatocellular carcinoma and dysplastic nodules. *Adv Ultrasound Diagn Ther* 1:14–20
17. Li F, Li Q, Liu Y et al (2020) Distinguishing intrahepatic cholangiocarcinoma from hepatocellular carcinoma in patients with and without risks: the evaluation of the LR-M criteria of contrast-enhanced ultrasound liver imaging reporting and data system version 2017. *Eur Radiol* 30:461–470
18. Kim YY, Kim MJ, Kim EH, Roh YH, An C (2019) Hepatocellular carcinoma versus other hepatic malignancy in cirrhosis: performance of LR-RADS version 2018. *Radiology* 291:72–80
19. Narsinh KH, Cui J, Papadatos D, Sirlin CB, Santillan CS (2018) Hepatocarcinogenesis and LI-RADS. *Abdom Radiol (NY)* 43:158–168
20. Yang D, Li R, Zhang XH et al (2018) Perfusion characteristics of hepatocellular carcinoma at contrast-enhanced ultrasound: influence of the cellular differentiation, the tumor size and the underlying hepatic condition. *Sci Rep* 8:4713
21. Feng Y, Qin XC, Luo Y, Li YZ, Zhou X (2015) Efficacy of contrast-enhanced ultrasound washout rate in predicting hepatocellular carcinoma differentiation. *Ultrasound Med Biol* 41:1553–1560
22. Lee HS, Kim MJ, An C (2018) How to utilize LR-M features of the LI-RADS to improve the diagnosis of combined hepatocellular-cholangiocarcinoma on gadoxetate-enhanced MRI? *Eur Radiol* 29:2408–2416

Publisher's note Springer Nature remains neutral with regard to jurisdictional claims in published maps and institutional affiliations.